

Article

Particle Size, Effects of Distance and Height from Source, Carbon Components, and Source of Dust in Nanchang, Central China

Hong Huang¹, Zihan Huang¹, Changwei Zou^{1,*}, Yuan Tang¹, Jianlong Li¹ , Chenglong Yu² and Fangxu Zhu³

¹ Key Laboratory of Poyang Lake Environment and Resource Utilization, Ministry of Education, School of Resources & Environment, Nanchang University, Nanchang 330031, China; honghuang@ncu.edu.cn (H.H.); 405800210036@email.ncu.edu.cn (Z.H.); 5811121047@email.ncu.edu.cn (Y.T.); jlli@ncu.edu.cn (J.L.)

² School of Land Resources and Environment, Jiangxi Agricultural University, Nanchang 330045, China; hjclyu@jxau.edu.cn

³ No.270 Research Institute of Nuclear Industry, Nanchang 330200, China; zhufangxu@cnuc.cn

* Correspondence: cwzou@ncu.edu.cn

Abstract: Regional air quality and major sources can be reflected by dust. 87 dust samples in Nanchang (four residential areas and three roadside points) were collected, with particle size and carbon components determined to discuss the distribution characteristics and the sources. The distribution of dust particle size in different sampling areas was similar, composed mainly of particles larger than 10 μm (over 69.8%). Dust particle size showed a decreasing trend with increasing horizontal distance from the main road and vertical height from the ground. EC in road dust was higher than that in residential dust. EC outdoors was higher than EC indoors in the same area. OC in indoor dust was higher than that in atmospheric dust when there were obvious indoor OC emission sources. The main carbon fractions in residential dust were OC3 and EC1, and in road dust were EC2 and OC3. The distribution of carbon fractions showed that OC3 and EC2 were mainly affected by human activities and motor vehicle emissions, respectively. The ratio of OC/EC and SOC in dust decreased from autumn to winter. SOC in the dust of Nanchang was at a medium level compared to other cities/regions around world. Clustering analysis and principal component analysis indicated that combustion sources (coal and biomass combustion, etc.), motor vehicle exhaust sources (gasoline and diesel vehicles), and human sources (cooking fumes, cigarette smoking, etc.) were the main contributors to the carbon components in dust.

Keywords: dust; particle size; organic carbon (OC); elemental carbon (EC); carbon fraction



Citation: Huang, H.; Huang, Z.; Zou, C.; Tang, Y.; Li, J.; Yu, C.; Zhu, F. Particle Size, Effects of Distance and Height from Source, Carbon Components, and Source of Dust in Nanchang, Central China. *Atmosphere* **2024**, *15*, 133. <https://doi.org/10.3390/atmos15010133>

Academic Editor: Avelino Eduardo Saez

Received: 12 December 2023

Revised: 8 January 2024

Accepted: 17 January 2024

Published: 21 January 2024



Copyright: © 2024 by the authors. Licensee MDPI, Basel, Switzerland. This article is an open access article distributed under the terms and conditions of the Creative Commons Attribution (CC BY) license (<https://creativecommons.org/licenses/by/4.0/>).

1. Introduction

Particulate matter is still one of the main atmospheric pollutants in China, even though China's nationwide $\text{PM}_{2.5}$ (particulate matter with an aerodynamic diameter not exceeding 2.5 μm [1]) concentration has dropped significantly since the implementation of the Action Plan for Prevention and Control of Air Pollution (2013–2017) and the Three-Year Action Plan for Winning the Battle for the Blue Sky (2018–2020) [2–4]. At present, the $\text{PM}_{2.5}$ concentration in some cities in China sometimes exceeds 10 $\mu\text{g}/\text{m}^3$, the annual standard limit recommended by the World Health Organization (WHO) [5], and there is still a long way to go in the prevention and control of atmospheric particulate matter in China. Dust is a kind of particulate matter that naturally settles on the surface under the influence of gravity in the atmospheric environment, and it has a wide range of particle size distribution that varies from <63 μm to >2 mm [6]. Dust is an important medium for the transport of heavy metals, organic matter, and other substances and energy. Some studies have found that the rate of mass transfer is higher in cases with finer particles, thus making hazardous components contained in these finer particles more available. The fraction of very small particles in house dust (for example, $\text{PM}_{2.5}$) is especially important with respect to inhalation after resuspension [7]. The particle size and chemical components of dust

can reflect the complacent and main sources [8,9]. A systematic study of the deposition, sources, chemical components, and influencing factors of dust in different regions is of practical significance for understanding the current status of regional ambient air quality, and it is also of great importance for studying the geographical distribution characteristics of dust.

Currently, there are some relevant studies in the field of atmospheric dust at home and abroad. One study investigated the depositional sorting characteristics and the depositional sorting process of atmospheric dust in the vertical direction from the perspective of deposition dynamics of the airflow field, which revealed the formation process and particle size distribution law of wind deposits [10]. Gupta's team studied the dustfall flux of atmospheric dustfall in Delhi, India, and the effects of cations and ions on plant leaves, and found that concentrations of chlorophyll and carotenoid decreased with the increase in dustfall flux, while the concentrations of proline and ascorbic acid increased with the increase in dustfall flux [11]. BiBi et al. conducted a continuous study on the North African coast of the Mediterranean Sea, and determined the spatial-temporal variation trend of atmospheric dust load and sedimentation flux [12]. Based on the application of the turbulent diffusion theory of the atmospheric boundary layer and the adsorption model of gas by porous solid particles, some scholars have analyzed the typical dust conditions of dust storm events in the Eastern Mediterranean. It was shown that, during the dust event, the concentration of PM₁₀ in the mildly stable atmospheric surface layer was higher than that in the neutral stable atmosphere, and the concentration of nitrate was strongly dependent on the concentration of atmospheric dust particles. The results of these studies provide a reference for the quantification of the effects of atmospheric dust on climate as well as health risks [13]. However, the current research direction is mainly oriented towards atmospheric dustfall fluxes, and less attention is paid to indoor dust compared to atmospheric dustfall. Additionally, there is a lack of attention given to the particle size and chemical composition of dustfall in different microenvironments, especially the carbon composition. Moreover, carbonaceous aerosols pose adverse impacts on human health [14,15]. The impacts of carbonaceous aerosols on the environment, climate, and human health highly rely on their size distribution and components [16]. Compared with larger particles, ultrafine particles (UFPs, with a particle diameter less than 0.1 μm) have greater adverse effects on human health because they can easily penetrate alveoli or translocate to circulation and reach many important organs, including the liver, heart, and nervous system [17,18]. About 60% of the OC in ultrafine particles can be deposited in the alveoli. Diesel EC mainly can be deposited in the alveolar region. It is necessary to control the emission of ultrafine particles and carbon components [19].

Due to regional climatic factors and early national industrial layout [20], studies on dust in China mainly focus on the northwest desert area [21–23], the northeast area [24,25], and the southeast coastal cities [26–28], while studies on dust in central China are limited. As a typical provincial capital city in central China, Nanchang has a mild and humid climate, strong light radiation, and sufficient precipitation, which provide active conditions for atmospheric photochemical reactions [29]. In recent years, the rapid development of Nanchang city and its surrounding industries, the increasing number of motor vehicles, and the current situation of the coal-based energy structure make the regional air pollution prevention and control situation still grim. Taking the atmospheric dust from Nanchang City as the research object, in-depth and detailed research on the composition, distribution, and source of regional dust can provide important basic data and a scientific basis for discussing the influential factors of regional dust and air pollution prevention and control.

Different sources and environmental backgrounds lead to differences in the particle size and chemical composition of dust samples. Different particle sizes and chemical compositions of dust have different impacts on the atmospheric environment and human health. In this study, indoor dust and outdoor dust in four residential areas and by the side of three roads in Nanchang were collected. The particle size of dust and the carbon components in the dust were measured and analyzed, and the influencing factors of dust

particle size and carbon composition (direction, distance, height from the emission source, etc.) were explored. The contents and results of the article will provide an important scientific basis for the prevention and control of airborne particulate matter pollution in Nanchang City and other regions.

2. Materials and Methods

2.1. Sample Collection

Indoor and outdoor dust samples were collected in September, October, and November 2021 in four residential areas (sampling areas A, B, C, and D) in Nanchang City, and road dust was collected in October 2021 beside three roads at sampling points E, F, and G in the city. Sampling area A was student dormitory buildings in a university, and sampling areas B, C, and D were residential communities, both with high occupancy rates, and sampling points E, F, and G were located on the roadside of major roads in the city. The location of each sampling area/point is shown in Figure 1.

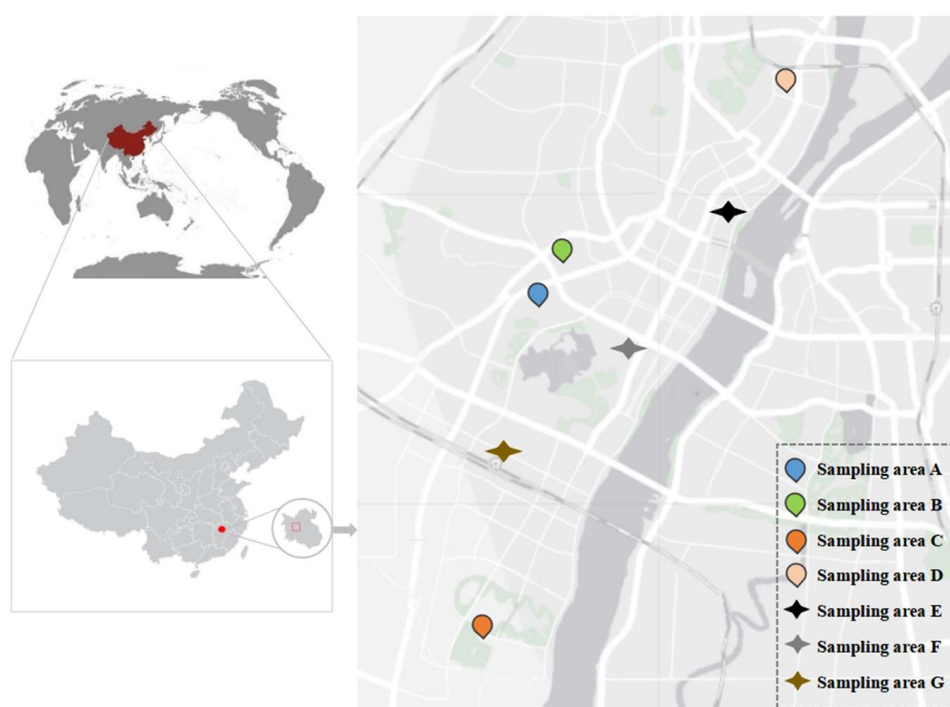


Figure 1. The location of sampling areas A/B/C/D and sampling points E/F/G.

Sampling area A and sampling area B were residential areas located by the side of a main traffic road (urban expressway with a traffic flow of about 40,000 vehicles/day), and dust sampling points in the two areas were set according to different horizontal distances from the main road. Dust samples were collected inside and outside of buildings (Buildings No.18, No.17, No.16, No.12, No.11, and Art Building) at sampling area A and inside and outside of buildings (Buildings No.1, No.17, No.18, No.25, and No.31) at sampling area B (Figure 2). Sampling area C was a modern commercial and residential complex community, and sampling area D was a simple residential community with an extremely low commercial atmosphere. In sampling areas C and D, respectively, 32-story high-rise residential buildings were selected as sampling sites, and samples of dust were collected from 1F, 4F, and every subsequent four floors of the sampled building at different vertical heights.

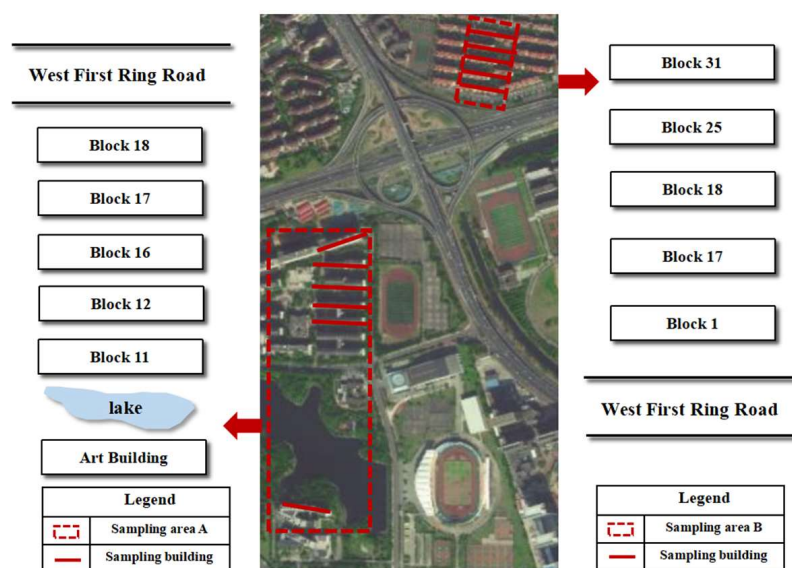


Figure 2. The location of sampling points with different horizontal distances from the main road in sampling areas A and B.

Vehicle volumes in sampling areas E, F, and G were 11,040, 59,160 and 55,280 vehicles per day, respectively [30].

One month before the formal collection of indoor dust and atmospheric dust samples from sampling areas A, B, C, and D, the sampling site was thoroughly cleaned one month prior to sampling to ensure that the collected samples were fresh dust deposited within the last month. Dust samples were collected using specifically designed and clean brushes (with stainless steel bristles) on the indoor and hallway door tops, window sills, handrails, and cabinet tops of the sampling areas (1–2.5 m above floor level). Dust that had fallen on the outdoor air conditioning machine, leaf, pipe surfaces, etc. (1–2.5 m from the ground) were collected, and the dust samples on these surfaces were mixed. The mixed samples were packed into plastic self-sealing bags and then sealed and preserved. Road dust samples were collected by direct sweeping with as little flow as possible under low wind conditions and no interference from rainfall. In the sampling process, we aimed to avoid obvious large particles and impurities, using a clean brush to sweep the dust samples into sealed bags to avoid light preservation. After sampling, the atmospheric dust samples were processed in a timely manner, and the related experimental preparations were carried out [31].

2.2. Sample Pretreatment

2.2.1. Sample Pretreatment Method for the Determination of Dust Particle Size

The collected dustfall samples were freeze-dried by vacuum, debris was removed, and the samples were weighed. A 0.1 g sample was added to 10 mL 10% H_2O_2 solution and 10 mL 10% HCl solution and stood for 12 h, then centrifuged at $4500\times$ rpm for 12 min. A 0.05 mol/L sodium hexametaphosphate solution was used as a dispersant to determine the dust particle size [32].

2.2.2. Sample Pretreatment Method for the Determination of Carbon Components in Dust

A 0.1 g sample was added to 10 mL 2 mol/L HCl solution and centrifuged at $4500\times$ rpm for 12 min after 24 h of reaction at room temperature. The centrifuged solid sample was added to a mixture of 15 mL HCl solution and HF solution (6 mol/L HCl solution and HF solution mixed at a ratio of 1:2). After reacting at room temperature for 24 h, the mixed solution was centrifuged at $4500\times$ rpm for 12 min. The centrifuged solid sample was added to 10 mL 4 mol/L HCl solution and centrifuged at $4500\times$ rpm for 12 min after reacting at 60°C for 24 h. The purpose of the tertiary acid treatment is to

remove carbonic acid and metals and dissolve silicates and residual metals and minerals, respectively. The acid-treated samples were filtered by vacuum pump onto the quartz filter membrane, which was cleaned by heat treatment. The quartz filter membrane, which retained the dust samples after acid treatment, was freeze-dried by vacuum and stored in cold storage until carbon component determination [33].

2.3. Sample Determination

The particle size of the dust was determined using the Mastersizer 3000 laser particle size analyzer, which has high resolution and sensitivity, suitable for the determination of wet and dry samples, with a range of 0.01–3500 μm .

The carbon components in the dust were determined using the Model 2015 thermo-optical carbon analyzer developed by the Desert Research Institute of the United States. The thermal-optical carbon analysis is based on the different order of oxidation of OC and EC at different temperatures and atmospheres, and the IMPROVE (Interagency Monitoring of Protected Visual Environments) temperature program was adopted [29].

2.4. Quality Control

The blank quartz filter was sealed with tin foil and pyrolyzed in a Muffle furnace at 800 $^{\circ}\text{C}$ for 3 h to remove possible residual organic matter on the blank filter. After vacuum freeze-drying, the quartz filter membrane was left to stand for 48 h and then weighed. The carbon analyzer was calibrated to CH_4/He standard gas at a 1:19 ratio [34].

3. Results and Discussion

3.1. Particle Size Distribution of Dust

3.1.1. Particle Size of Indoor and Outdoor Dust in Different Areas

The particle size of the dust samples was divided into five particle size ranges: {0, 2.5}, {2.5, 10}, {10, 50}, {50, 100}, and {100, 3000} μm , given the particle size of dust and its impact on human health. The particle size range distribution of all (indoor and outdoor) dust samples at sampling areas A, B, C, and D is shown in Figure 3a. The particle size range distribution of indoor or outdoor dust samples at sampling areas A and B is shown in Figure 3b.

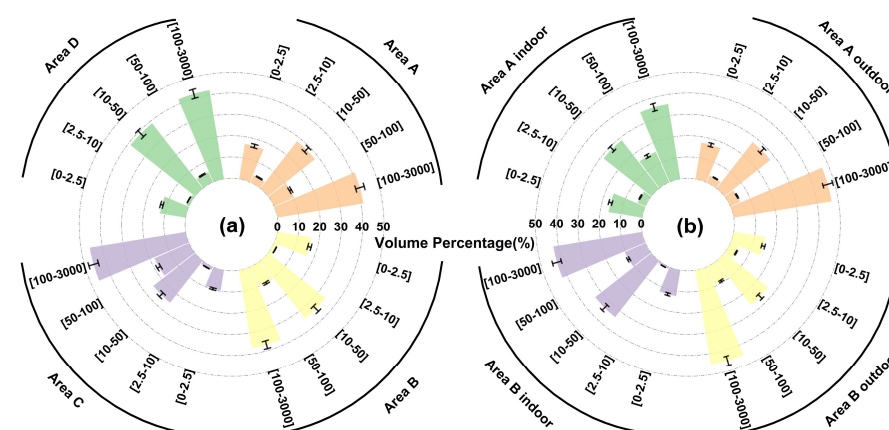


Figure 3. Particle size range distribution of dust in (a) four residential sampling areas and a comparison of the indoor and outdoor dust particle size range distribution in (b) sampling areas A and B.

As can be seen from Figure 3a, the particle size range of dust at sampling areas A, B, C, and D presented a high, low, high, low, and high pattern across the five particle size ranges ({0, 2.5}, {2.5, 10}, {10, 50}, {50, 100}, and {100, 3000} μm). The percentage of dust particles in the range of {0, 2.5}, {10, 50}, and {100, 3000} μm was 9.7–16.6%, 25.0–38.7%, and 37.2–45.9%, respectively, showing an increasing distribution. The percentage of dust particles in the range

of {2.5, 10} and {50, 100} μm was 1.5–3.8% and 5.3–17.9%, respectively. On the whole, dust from Nanchang City was composed of particles with a size greater than 10 μm (over 69.8%).

According to Figure 3b, the particle size distributions of indoor and outdoor dust at sampling areas A and B were similar to the overall dust particle size distributions in the sampling areas, and the dust particles were mainly located in the range of {10, 50} and {100, 3000} μm . The percentage of large-sized particles ({100, 3000} μm) in outdoor dust at sampling area A was 46.8%, which was significantly higher than the distribution of particles in the range of {100, 3000} μm in indoor dust in this sampling area (35.6%). This was due to the renovation construction works carried out by the periphery of Building No.16 in sampling area A during the sampling period. The generation of construction dust led to an increase in the cumulative level of coarse particles in the outdoor dust, indicating that construction dust can have a significant impact on the particle size distribution of dust. The difference between indoor and outdoor dust particle size at sampling area B was that the proportion of dust distributed in the range of {10, 50} and {50, 100} μm was significantly higher indoors than outdoors, which might be due to the presence of frequent anthropogenic sources such as cigarette smoking in the vicinity of the sampling site in sampling area B [35].

3.1.2. Effects of Distance from Road on Particle Size Distribution of Indoor and Outdoor Dust

The sampling locations of the Art Building and student dormitories No.11, No.12, No.16, No.17 and No.18 in sampling area A and Residential Buildings No.31, No.25, No.18, No.17 and No.1 in sampling area B were located on both sides of the main traffic artery of the Qianhu Interchange. The horizontal distances from the artery were distributed in a straight line, with student dormitories No.18 and Residential Building No.1 being the closest to the main artery. Atmospheric dust samples collected from indoor and outdoor sampling locations in the two sampling areas were analyzed and discussed in terms of the percentage of dust particle size range distribution in each particle size range.

The distribution of atmospheric dust particle size in sampling areas A and B along with the horizontal distance from the main road is shown in Figure 4.

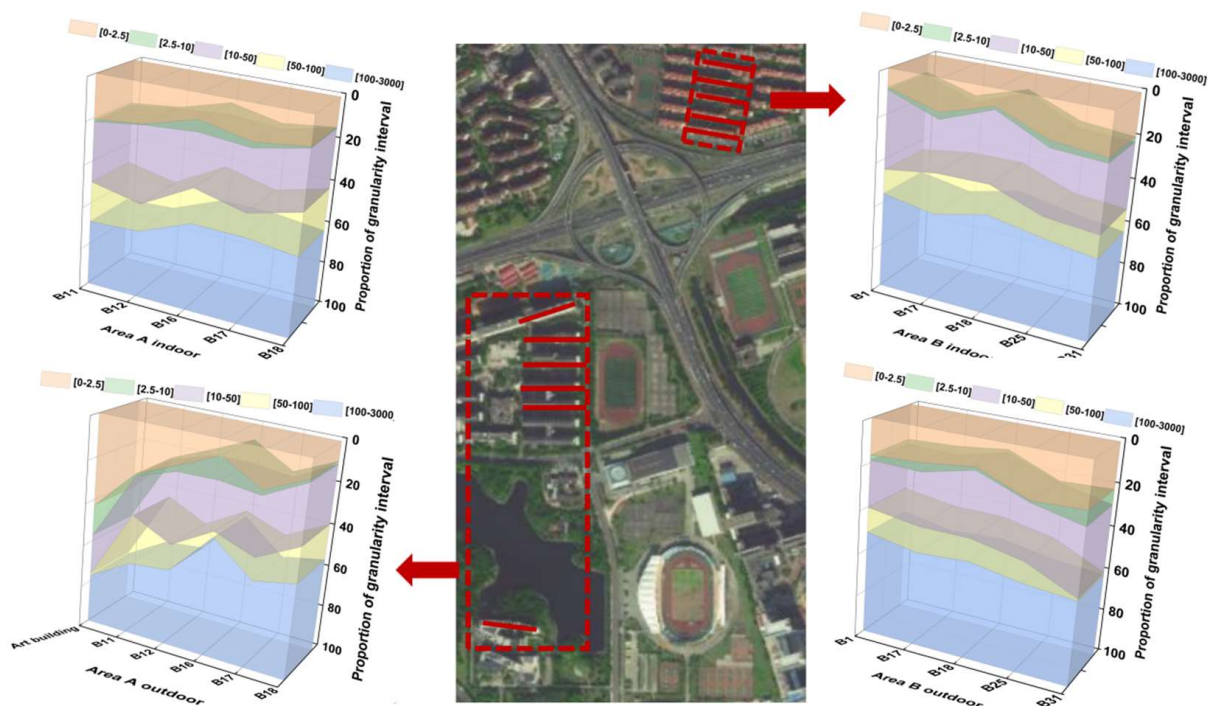


Figure 4. Particle size range distribution of atmospheric dust in sampling areas A and B with the horizontal distance from the main road.

According to Figure 4, during the sampling period, the distributions of atmospheric dust particles at the outdoor sampling locations of Buildings No.18, No.17, No.16, No.12, No.11, and the Art Building in sampling area A were 45.2%, 41.5%, 56.3%, 36.0%, 34.0%, and 23.0%, respectively, in the particle size range of greater than $100\ \mu\text{m}$. As mentioned above, renovation construction works were carried out on the periphery of Building No.16, which led to the generation and deposition of a large amount of coarse particulate matter due to the dismantling and handling of construction materials and part of the outdoor construction process, resulting in a significantly large percentage of large particulate matter with a particle size of $100\ \mu\text{m}$ or more in the vicinity of the building. Green belts and dust removal plants can play an active role in controlling road dust, as pointed out by Gondwal T. K. et al. [36]. The Art Building, which was separated from the student dormitory buildings by a lake and a large green belt, had a smaller proportion of coarse particulate matter than the other sampling sites, consistent with Gondwal T. K.'s study. The particle size distribution of indoor dust was less affected by construction activity than that of outdoor dust, due to the fact that the majority of dormitory doors and windows were closed during the construction period, which was the summer vacation period. In addition, as the horizontal distance from the main road increased, the distribution of atmospheric dust particles showed a tendency to reduce the percentage of the overall distribution in the particle size section of more than $100\ \mu\text{m}$ and to increase the percentage of the overall distribution in the particle size range of less than $10\ \mu\text{m}$.

The proportion of atmospheric dust particles in the outdoor sampling locations in sampling area B decreased from 48.1% to 37.1% in the size range larger than $100\ \mu\text{m}$ and increased from 16.5% to 19.8% in the size range less than $2.5\ \mu\text{m}$. The size distribution of indoor dust in the sampling area exhibited a similar distribution to that of outdoor dust. The farther away from the road, the smaller the average particle size of the dust at the sampling point. In summary, as the horizontal distance from the main road increased, the particle size of both indoor and outdoor dust tended to be smaller, as coarse particles settled more near the main road.

3.1.3. Effects of Height on Particle Size Distribution of Indoor Dust

As described in Section 2.1, the sampling locations in sampling areas C and D were high-rise residential buildings in a modern residential community, with a floor structure of 32 floors and a height of about 3 m per floor. Indoor dust sampling was conducted on the 1st, 4th, 8th, 12th, 16th, 20th, 24th, 28th, and 32nd floors (1F, 4F, 8F, 12F, 16F, 20F, 24F, 28F, and 32F) of the sampling building, respectively.

The particle size distribution of indoor dust at each sampling location in the sampling buildings of sampling areas C and D is shown in Figure 5.

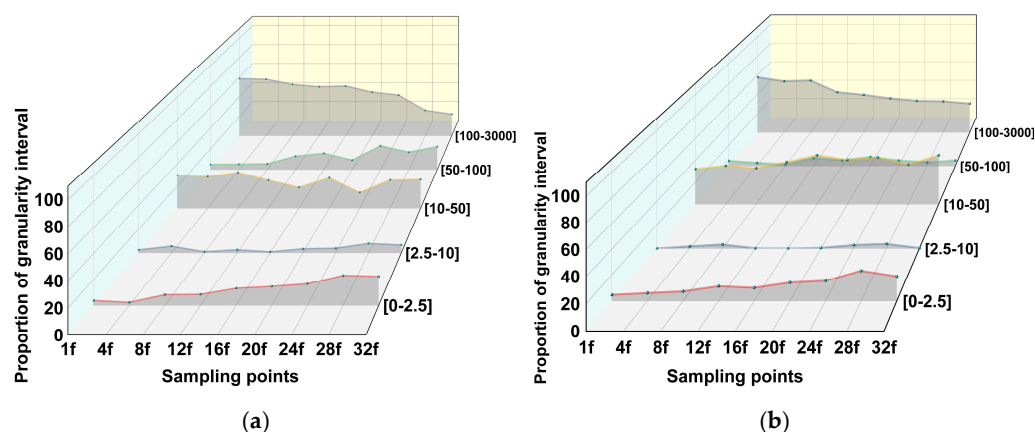


Figure 5. Particle size range distribution of indoor dust in (a) sampling area C and (b) sampling area D with the vertical height change.

As shown in Figure 5a, from 1F to 32F, the proportion of particles in the range of {1, 2.5} μm showed an increasing trend, while the proportion of particles in the range of {100, 3000} μm showed a gradual decreasing trend. The proportion of particles in the range of {2.5, 10} and {50, 100} μm showed fluctuations on different floors, while the proportion of particles in the range of {10, 50} μm showed a weak increasing trend. The variation trend of indoor dust particles in the range of {1, 2.5}, {2.5, 10}, {50, 100}, and {100, 3000} μm with floor height change in sampling area D was similar to the variation trend of dust particles in the four ranges with floor height change in sampling area C. The main difference lies in the distribution characteristics of particles in the range of {50, 100} μm on different floors.

According to Figure 5b, for the dust particles on different floors in sampling area D, the proportion of particles in the range of {50, 100} μm showed fluctuations on different floors, not showing a weak increasing trend like that in sampling area C. The indoor dust particles on low floors (1–8F) were mainly distributed in a particle size range larger than 100 μm . The indoor dust particles on middle floors (12–20F) were mainly distributed in the 10–100 μm particle size range, and the percentage of particles with a particle size larger than 100 μm decreased but the percentage was still large. The indoor dust particles on high floors (24–32F) were mainly particles with a particle size smaller than 50 μm , while the percentage of particles distributed in the 100 μm and above particle size range decreased but still occupied a certain percentage.

In summary, with the increasing vertical height from the ground, the average particle size of indoor dust showed a decreasing trend.

3.2. Distribution of Carbon Components in Dust

3.2.1. Distribution of OC and EC in Dust

OC and EC in Dust of Different Sampling Areas

The analyzer applies the thermal–optical reflectance (TOR) method under the Interagency Monitoring of Protected Visual Environments (IMPROVE_A) protocol. Each sample was heated to produce four OC fractions (OC1, OC2, OC3, and OC4 at temperatures of 120, 250, 450, and 550 $^{\circ}\text{C}$ in a non-oxidizing He atmosphere) and three EC fractions (EC1, EC2, and EC3 at 550, 700, and 800 $^{\circ}\text{C}$ in an oxidizing atmosphere of 2% O₂ and 98% He) [37].

The average mass concentrations of OC and EC in dust and OC/EC ratios in different sampling areas are shown in Figure 6.

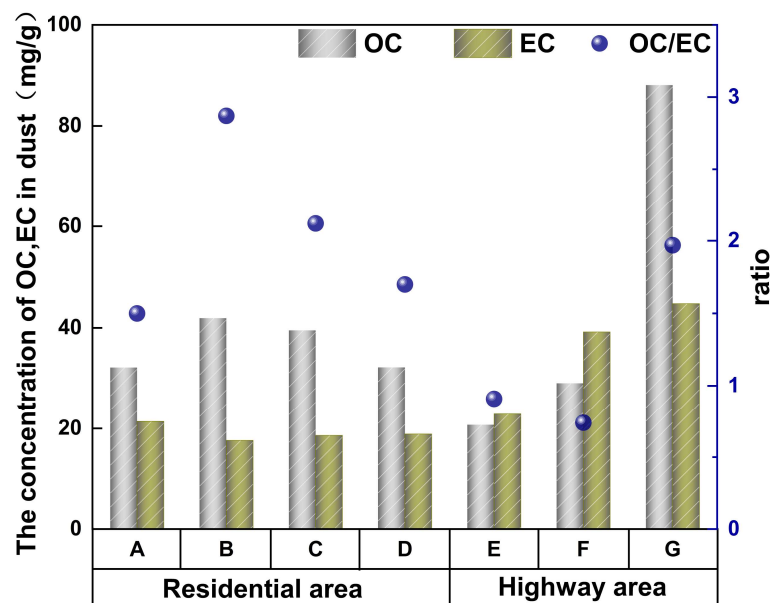


Figure 6. Average mass concentrations of OC and EC in dust and OC/EC ratios in different sampling areas/points.

The average mass concentrations of OC in the dust of residential sampling areas ranged from 32.2 to 41.9 mg/g. There was no indoor cooking source for dust in sampling area A, and the mass concentration of OC in this sampling area was lower than that in the other three residential areas. The mass concentration of OC in the dust of sampling area B was higher, presumably due to anthropogenic activities such as heavy smoking in its centralized recreation room in Building No.18, in addition to culinary sources. The mass concentration of EC in the dust of the four residential areas ranged from 18.6 to 21.4 mg/g, among which the mass concentration of EC in sampling area A was the highest. As mentioned above, building decoration work was carried out in Building No.16 in sampling area A during the sampling period. At the same time, there were many heavy trucks transporting construction materials entering and exiting, driving, and braking, resulting in a large number of carbon smoke particles deposited on the road surface. The EC content in the road dust of sampling points (E, F, and G) (22.9–44.8 mg/g) was higher than that in residential areas. Sampling point E was located near the Ganjiang River, and the adjacent road was four lanes with a moderate amount of traffic of motor vehicles. Therefore, EC content in road dust in this point was just slightly higher than that in residential dust. A large number of motor vehicles passed through sampling points F and G, and the EC content in the road dust at these two sampling points was significantly higher than that in residential dust. In addition, not only the EC content but also the OC content in the road dust at sampling point G was the highest, attributed to the fact that sampling point G was not only located next to the main traffic road but also next to a bus stop near the main traffic road. There was a braking operation before the vehicle stopped at the stop. Moreover, there were a lot of pedestrians waiting and smoking frequently at the bus stop, bringing a certain amount of OC content, which led to the absolute content of OC and EC in the road dust at sampling point G being higher than that of OC and EC in the road dust at sampling point E.

The OC/EC ratio in the dust of four residential sampling areas ranged from 1.50 to 2.87 (average 2.0), and the ratio of OC/EC in road dust at three road dust sampling points ranged from 0.74 to 1.97 (average 1.2), indicating that the OC/EC ratio in residential dust was slightly higher than that in road dust, mainly due to the increase in EC content in road dust. The OC/EC ratio (1.97) in the road dust at sampling point G was obviously higher than that in the road dust at sampling points E (0.91) and F (0.74), which is also attributed to the fact that the road dust at sampling point G was affected not only by vehicle exhaust traffic source but also by the cigarette source, and the OC/EC characteristic ratio of particulate matter emitted by the cigarette combustion source was high [38].

Comparison of OC and EC in Indoor Dust and Outdoor Dust in the Same Area

The mass concentrations of OC and EC and OC/EC ratios in indoor and outdoor dust at sampling areas A and B are shown in Figure 7.

Generally, the mass concentrations of OC in dust are easily influenced by domestic emission sources from nearby households. Figure 7 shows that the concentration of OC in indoor dust (average 31.6 mg/g) was slightly less than that in outdoor dust (average 32.7 mg/g) at sampling area A. The indoor OC content (average 56.4 mg/g) at sampling area B was significantly higher than that of outdoors (average 21.0 mg/g). It was found that the comparison of OC in indoor and outdoor dust was not clear in terms of what was larger or smaller. In the absence of specific indoor sources, the concentrations of OC in outdoor dust were comparable to that of OC in indoor dust, but when there were significant indoor sources (cigarettes, etc.), indoor dust OC concentrations were significantly greater than outdoor dust OC concentrations. For the concentration of OC in indoor dust at sampling area B, the OC mass concentration of indoor dust in Building 18 was the highest (112.0 mg/g). The occupancy rate of Building No.18 was high, and the first floor of this building was occupied as an elderly activity center and a chess and card room. Indoor activities, such as smoking, closing doors and windows, using air conditioning, and cooking, increased the concentration of OC in indoor dust. This study suggests that indoor

environments should be regularly ventilated and cleaned, and indoor smoking should be avoided as much as possible to reduce the concentration of indoor dust and its components, such as OC, reducing the health risk for indoor populations.

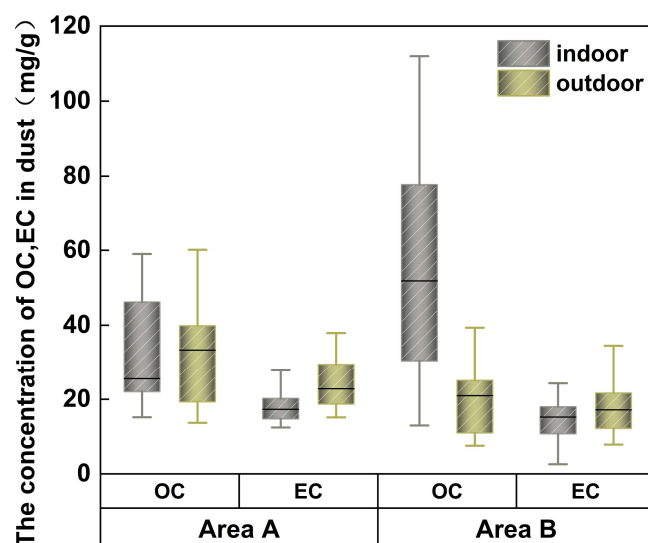


Figure 7. Mass concentrations of OC and EC and OC/EC ratios in indoor and outdoor dust at sampling areas A and B.

EC is a kind of primary pollutant emitted directly from the combustion of biomass or fossil fuels and is often used as an indicator of motor vehicle emission source [39]. Sampling areas A and B are located on both sides of the same main road, adjacent to each other. The environmental background and emission sources of the two areas were basically the same, and EC in the dust of the two areas was significantly affected by motor vehicle exhaust emissions. According to Figure 7, it was found that the concentration of EC in indoor and outdoor dust in both sampling areas showed a pattern of higher outdoor concentrations than indoor concentrations. The average EC concentration in outdoor dust at sampling area A was 24.0 mg/g, while the average EC concentration in indoor dust was 18.8 mg/g. The average EC concentration in outdoor dust at sampling area A was 18.2 mg/g, and the average EC concentration in indoor dust was 15.0 mg/g.

In conclusion, OC content in indoor dust of the residential area was higher than that in atmospheric dust when there were obvious indoor OC emission sources. On the contrary, EC content in indoor dust of the residential area was mainly affected by surrounding outdoor primary emission sources.

3.2.2. Distribution of 7 Carbon Fractions in Dust

Carbon Fractions in Dust at Different Sampling Areas/Points

The percentages of the seven carbon fractions (OC1, OC2, OC3, OC4, EC1, EC2, and EC3) in the mixed indoor and outdoor dust samples from four residential areas and the road dust samples from three roadway areas are shown in Figure 8.

As shown in Figure 8, the percentage of carbon fractions in the mixed samples of indoor and outdoor dust in the residential area is in the following order from large to small: OC3 (over 40%) > EC1 (over 20%) > EC2&OC2&OC4 (6.9–13.4%) > EC3&OC1 (below 2.5%). The high proportion of OC3 to total carbon (TC) in dust from sampling area A (over 40%) and the high proportion of OC3 to TC in dust from sampling area B (over 50%) reflect the significant impact and contribution of human sources on OC3. The percentage of carbon fraction to TC in outdoor road dust at sampling points (E, F, G) of roadside areas is different from that in residential areas. At sampling points E and F, the order of carbon fractions in road dust from high to low is EC2 (over 36%) > OC3 (25.6–29.2%) > EC1&OC4 (14.5–16.3%) > OC2 (2–2.5%) > EC3&OC1 (below 1%). Com-

pared to the distribution of EC2 in residential dust, the proportion of EC2 in road dust is significantly higher. Liu et al. [19] collected the particulate matter emitted by five typical vehicle types (including light gasoline vehicles, heavy gasoline vehicles, diesel buses, light diesel vehicles, and heavy diesel vehicles), determined the mass concentration and emission factors of OC and EC, and calculated the sedimentation flux of carbon aerosols of different particle sizes in the human respiratory system using a respiratory sedimentation model. EC2 was found to dominate the carbon fractions of particulate matter emitted by all types of vehicles except light gasoline vehicles, and EC was mainly deposited in the alveolar region [19]. The high proportion of EC2 in road dust at sampling points E and F of this study is consistent with the findings of Liu et al., and also indicates that special attention should be paid to the control of particulate matter emission sources in the indoor environment of roadside areas to reduce and avoid the emission and impact of diesel EC. While the distribution of carbon fractions in the road dust at sampling point G, OC3 (48.5%) > EC1 (21.5%) > EC2&OC4 (11.7–13.3%) > OC2 (4.4%) > EC3&OC1 (below 1%), is similar to that of residential sampling areas, which may be related to the smoking behavior of a large number of passengers diverted from the high-speed railway station to the bus stop, as mentioned in Section 3.2.1.

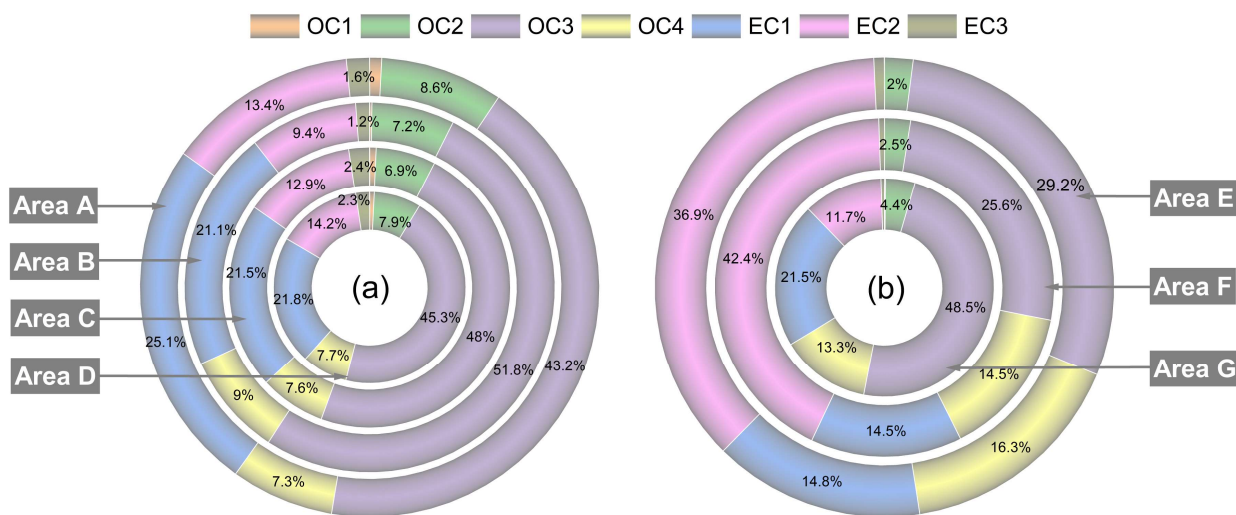


Figure 8. The percentages of carbon fractions in TC in dust at (a) residential sampling areas and (b) roadside sampling points.

In summary, the distribution of carbon fractions in indoor and outdoor dust samples in residential areas was OC3 > EC1 > EC2&OC2&OC4 > EC3&OC1, with OC3 dominating in TC, and the distribution of carbon fractions in road dust mainly originating from vehicle exhaust is EC2 > OC3 > EC1&OC4 > OC2 > EC3&OC1, with EC2 accounting for a great portion of TC.

Comparison of Carbon Fractions in Indoor and Outdoor Dust in the Same Area and the Differences of Carbon Fractions in Different Months

The distribution of the seven carbon fractions in indoor and outdoor dust at sampling areas A and B in September, October, and November is shown in Figure 9.

According to Figure 9a, the distribution of the seven carbon fractions in indoor dust at sampling area A was OC3 (38.1–40.4%) > EC1 (24.2–27.6%) > EC2&OC2&OC4 (5.4–15.7%) > EC3&OC1 (1.8–3.4%). The distribution of the seven carbon fractions in outdoor dust at sampling area A was OC3 (28.2–34.6%) > EC1 (26.0–30.4%) > EC2&OC2&OC4 (7.8–18.5%) > EC3&OC1 (1.6–3.2%). According to Figure 9b, the distribution of the seven carbon fractions in indoor dust at sampling area B was OC3 (40.4–55.4%) > EC1 (19.1–27.2%) > EC2&OC2&OC4 (6.3–11.7%) > EC3&OC1 (0.7–1.7%). The distribution of the seven carbon fractions in outdoor dust at sampling area B was OC3 (41.3–47.6%) > EC1

(18.3–33.6%) > EC2&OC2&OC4 (5.2–15.8%) > EC3&OC1 (0.9–2.4%). The distribution of the seven carbon fractions in indoor and outdoor dust showed certain differences. The total of four OC fractions of indoor dust accounted for a higher proportion (62.2% on average) than that of outdoor dust (60.2% on average), with OC3 accounting for the most (average of 44.0% indoors vs. 39.4% outdoors). Instead, the total of three EC fractions of outdoor dust accounted for a higher proportion (39.2% on average) than that of indoor dust (37.8% on average), with EC1 accounting for the most (average of 26.5% outdoors vs. 22.5% indoors). The above differences of carbon fractions between indoor and outdoor dust in residential areas indicated that OC (especially OC3) in indoor dust was more significantly affected by indoor human activities (smoking, etc.) than EC, and EC (especially EC1) in outdoor dust was more significantly affected by fossil fuel combustion such as motor vehicle exhaust emissions.

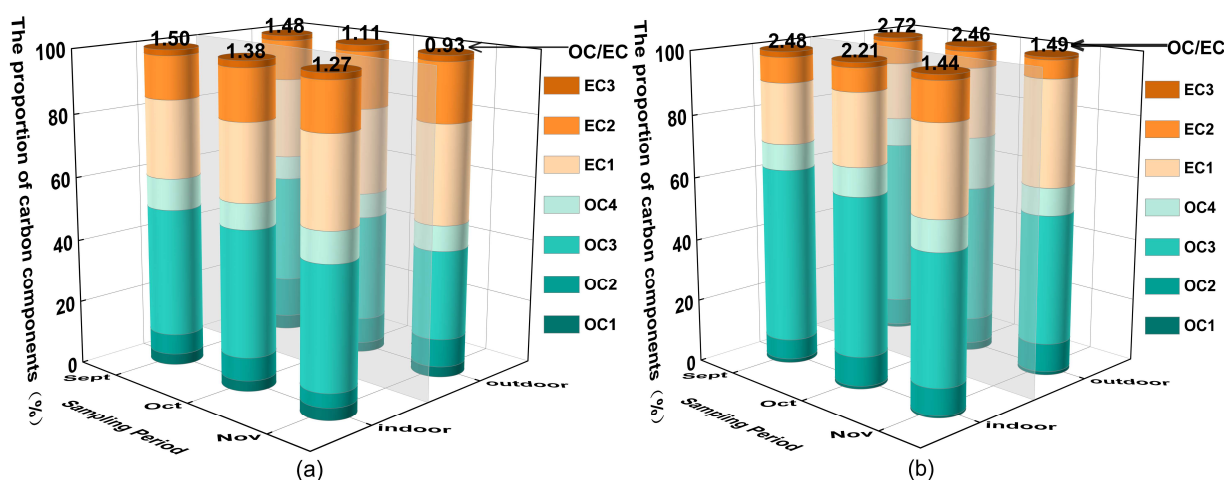


Figure 9. The proportion of the seven carbon fractions in indoor and outdoor dust in September, October, and November (a) at sampling area A and (b) sampling area B.

According to Figure 9a,b, during the seasonal transition from September, October to November, and autumn to winter, the proportion of OC (especially OC3) in indoor and outdoor dust samples from both sampling areas showed a decreasing trend, while the proportion of EC (especially EC1) showed an upward trend. OC includes primary organic carbon (POC) directly emitted from a primary source and secondary organic carbon (SOC) generated through the conversion of gaseous precursors in the atmosphere, where SOC is significantly influenced by factors such as light intensity [40]. From autumn to winter, the ratio of OC/EC in dust showed a downward trend. The average OC/EC in indoor dust at sampling area A in September, October, and November were 1.50, 1.37, and 1.27, and the OC/EC in outdoor dust at sampling area A in September, October, and November were 1.48, 1.11, and 0.93. The OC/EC in indoor dust at sampling area B in September, October, and November were 2.48, 2.21, and 1.44, and the OC/EC in outdoor dust at sampling area B in September, October, and November were 2.72, 2.46, and 1.69. During the transition from autumn to winter, the decrease in the proportion of OC and the gradual decrease in the OC/EC ratio were related to a decrease in temperature and light intensity. Mbengue et al. conducted a four-year high-frequency measurement analysis of OC and EC in Central Europe and showed that OC content and the OC/EC ratio continued to decrease from autumn to winter [41], which is consistent with the results of this study.

3.2.3. Distribution of Secondary Organic Carbon (SOC) in Dust

At present, the common method for calculating SOC in atmospheric particles is the EC tracer method, and the calculation formula is as follows [42]:

$$\text{SOC} = \text{OC} - \text{EC} \times (\text{OC}/\text{EC})_{\text{pri}}$$

where SOC is the estimated secondary organic carbon mass concentration in mg/g, and $(OC/EC)_{pri}$ is the OC/EC of a primary emission to the atmosphere.

The key to the EC tracer method is in determining the value of $(OC/EC)_{pri}$. The minimum R squared (MRS) method was used in this study to determine $(OC/EC)_{pri}$. MRS calculates a set of hypothetical $(OC/EC)_{pri}$ values and their corresponding SOC values. The $(OC/EC)_{pri}$ values that generate the minimum R^2 (SOC vs. EC) is considered the obtained $(OC/EC)_{pri}$, as shown in Figure 10.

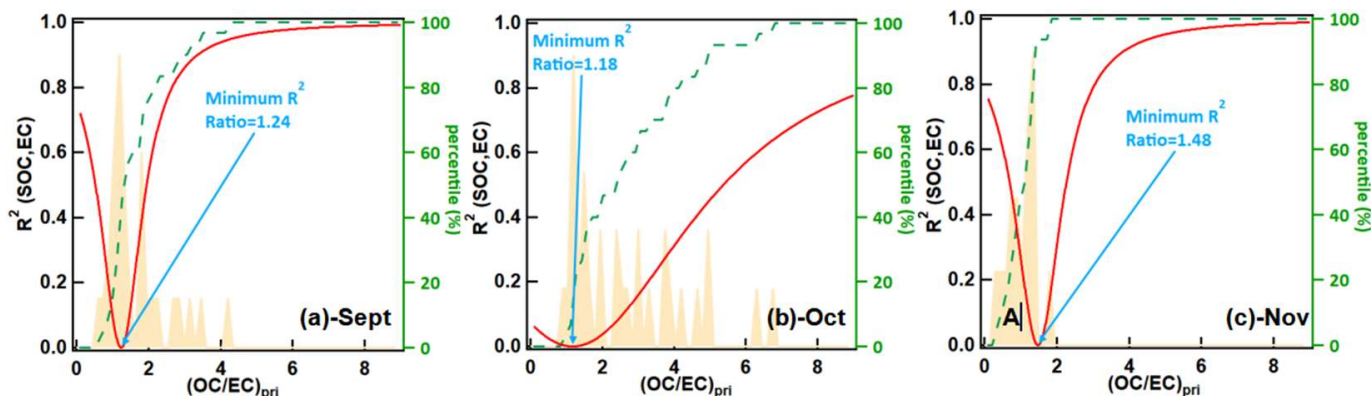


Figure 10. MRS Model fitting results of mixed dust samples at sampling areas A and B in September, October, and November.

According to the fitting results of the MRS Model using Igor Pro software (version 7.0, WaveMetrics, Inc., Lake Oswego, OR, USA) [43,44], the results of SOC in dust in September, October, and November are shown in Table 1.

Table 1. OC/EC and SOC in dust from Nanchang during the sampling period.

| Sampling Period | OC/EC | $(OC/EC)_{pri}$ | POC(mg/g) | SOC/(mg/g) | $(SOC/OC)/\%$ |
|-----------------|-----------------|-----------------|-----------|------------|---------------|
| September | 2.60 ± 0.28 | 1.24 | 17.30 | 14.60 | 45.78 |
| October | 2.22 ± 0.37 | 1.18 | 23.09 | 16.01 | 40.95 |
| November | 1.97 ± 0.23 | 1.48 | 30.91 | 8.90 | 22.35 |

According to Table 1, the calculated SOC in dust showed a similar distribution in September and October but was smaller in November. The proportion of SOC in OC in September, October, and November showed a descending trend. The climate in Nanchang city of Jiangxi Province is a subtropical monsoon climate with high temperatures in early autumn. According to a datasheet published in the Climate Bulletin of Jiangxi Province, the average temperature from September to November in Jiangxi Province was 27.8 °C, 21.7 °C, and 14.1 °C, respectively. The formation of SOC in air particle transformation is related to light intensity and temperature, and a temperature of 25 °C and a relative humidity of 78% were favorable for the generation of particulate SOC [45]. During the sampling period of this study in Nanchang, the average temperature in September and October was around 25 °C, and the SOC mass concentration and its percentage in OC were similarly high (22.35–45.78%). The average temperature in November was significantly lower compared to September and October; consequently, the SOC mass concentration and its percentage in OC were correspondingly lower in November, which was consistent with the research conclusion of William C. Porter et al. [45]. The ratio of OC/EC also followed the order September > October > November, indicating that the ratio of OC/EC can roughly reflect SOC generation to a certain extent.

In summary, there was a certain amount of SOC in the autumn atmospheric dust of Nanchang City, and as autumn moves towards winter, the OC/EC ratio and SOC in the

dust show a gradually decreasing trend. The reasons for this trend were multifactorial and may be related to factors such as gas–solid distribution, photochemical reactions, and meteorological conditions such as temperature and humidity.

3.2.4. Comparison of SOC and SOC/OC in Dust or PM_{2.5} between this Study and Other Regions

Table 2 lists the SOC content and SOC/OC ratio of atmospheric dust or PM_{2.5} in this study and some other areas reported. The results showed that the mass concentration of SOC in atmospheric dust or PM_{2.5} varied significantly among different regions (8.90–147.62 mg/g). The percentage of SOC in OC was between 20% and 70%, with an average of about 40%. In autumn (September to November), the percentage of SOC in OC in dust or PM_{2.5} in Nanchang, China, Chongqing, China, and Calabria, Italy, showed a decreasing trend over time.

Table 2. SOC and SOC/OC in dust or PM_{2.5} in this study and other regions.

| Location | Sample Type | Sampling Period | SOC/ (mg/g) | SOC/OC (%) | Reference |
|------------------------|---------------------------|-----------------------------|----------------|---------------|------------|
| Nanchang, China | dust | September 2020 | 14.60 | 46 | This study |
| | | October 2020 | 16.01 | 41 | |
| | | November 2020 | 8.90 | 22 | |
| Guangzhou, China | Outdoor PM _{2.5} | September 2012 | / | 48 | [46] |
| | | October 2012 | / | 40 | |
| | | November 2012 | / | 39 | |
| Calabria, Italy | Outdoor PM _{2.5} | September 2016 | 88.99 | 60 | [47] |
| | | October 2016 | 65.36 | 55 | |
| | | November 2016 | 36.93 | 37 | |
| Beijing, China | Indoor dust | December 2016 | 94.85 | 38 | [48] |
| Tianjing, China | Indoor dust | December 2016 | 84.41 | 42 | |
| Langfang, China | Outdoor dust | December 2016 | 147.62 | 37 | |
| Sichuan, China | Outdoor PM _{2.5} | Spring 2016 | 18.79 | 37 | [49] |
| | | Summer 2016 | 14.89 | 47 | |
| | | Autumn 2016 | 12.77 | 27 | |
| | | Winter 2016 | 34.89 | 41 | |
| Manora Peak, India | Outdoor PM _{2.5} | September– November 2006 | 24.81 | 28 | [50] |
| Abu Mountain, India | Outdoor PM _{2.5} | September– November 2006 | 27.13 | 20 | |
| Mexico City, Mexico | Outdoor PM _{2.5} | March 2006 | / | 74 | [51] |

Note: The mass concentration of SOC in some references was converted from mg/m³ to mg/g.

In this study, the SOC/OC ratio of the dust samples in Nanchang City was relatively low, significantly lower than in cities such as Calabria (Italy) (88.99 mg/g in September, 65.35 mg/g in October, and 36.93 mg/g in November 2016) and Mexico City (74.4 mg/g in March 2006). It was basically the same as that in Guangzhou, Beijing, Tianjin Langfang, and Sichuan, China, and slightly higher than that in Mount Manola and Mount Abu in India. It can be seen that the ratio of SOC/OC may have climate and regional correlations. As mentioned above, William C. Porter et al. regarded that the condition of 25 °C temperature and around 78% RH has a high potential for forming SOC [45]. Italy and Mexico have subtropical Mediterranean and tropical climates, respectively, with suitable autumn temperatures and relatively abundant rainfall, which is conducive to the production of SOC. The above-mentioned cities in China have a subtropical or temperate monsoon climate, with moderate autumn temperatures but low rainfall. The sampling points of Mount Manola (1950 m above sea level) and Mount Abu (1680 m above sea level) in India have higher elevations and lower temperatures. In addition, Abu Mountain is located in the semi-arid

region of western India, where there is a lot of sand and dust. Adverse climate conditions have led to the suppression of SOC generation in these two regions. In Table 2, the average value of SOC/OC in PM_{2.5} in each region is 42.5%, while this value is 37.7% in dust, which is the same as the study of Wang et al. [52]. In that study, the percentage of SOC in PM_{2.1} was higher than that in PM₁₀ for most of the sampling period, suggesting that SOC is more likely to be concentrated in fine particulate matter.

To sum up, the generation of SOC was affected by regional climate factors and particle size, and the SOC in dust from Nanchang was at a medium level around the world, which may be related to the climate conditions in Nanchang and the small number of large-scale emission sources, such as thermal power stations and heavy industry enterprises, in the surrounding areas.

3.3. Source Analysis of Carbon Components in Dust

3.3.1. Source Analysis of Carbon Fractions in Residential Area Dust Based on Cluster Analysis

Cluster analysis (CA) is a process of scientific distinction and classification according to the similarity between things. By defining a similarity coefficient between variables that represent the degree of similarity, variables are classified one by one according to the degree of similarity, and finally, a pedigree diagram can be formed to represent the degree of similarity [53]. In order to further analyze the source of dust from Nanchang City, IBM SPSS Statistics 27 software was used to conduct cluster analysis of seven carbon fractions in the dust samples from four residential sampling areas, and the results are shown in Figure 11.

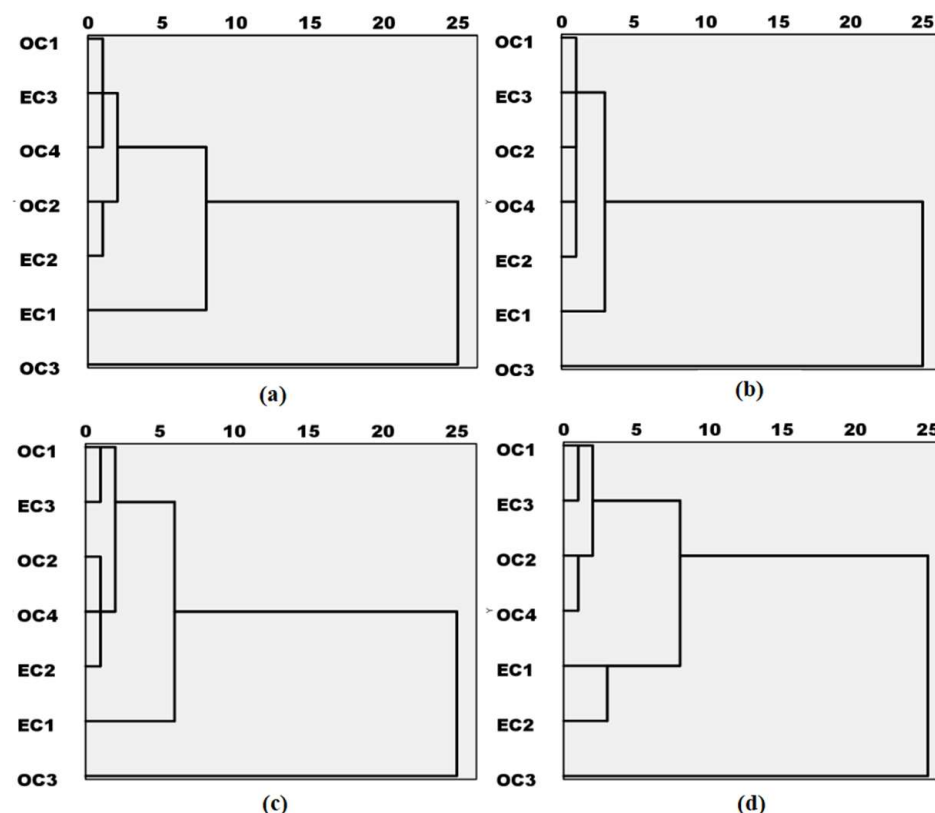


Figure 11. Cluster analysis of carbon fractions in dust at (a) sampling area A, (b) sampling area B, (c) sampling area C, and (d) sampling area D.

Studies show that OC1 mainly comes from biomass combustion, OC2 mainly comes from coal fuel combustion, and OC3 and OC4 are carbon components of road dust and anthropogenic sources. EC1 comes from automobile exhaust, and EC2 and EC3 come from diesel vehicle emissions. The emission sources of carbon fractions can be determined

according to the distribution characteristics of each carbon component [54–56]. As mentioned in Section 3.2.2, the percentages of carbon fractions in the dust of residential areas in Nanchang City show a consistent sequence: OC3 > EC1 > EC2&OC2&OC4 > EC3&OC1, indicating that the sources of carbon fractions in the dust from Nanchang are basically stable, which roughly reflects that major sources include anthropogenic sources and motor vehicle emissions, the contribution of exhaust emissions from gasoline vehicles is higher than that of diesel vehicles, followed by coal-fired emissions, and the contribution of biomass combustion is low.

According to the cluster analysis (Figure 11), the carbon fractions in the dust from Nanchang City can be divided into three categories. The first category comprises OC1, EC3, OC2, OC4, and EC2, and the main sources are a mixture of diesel vehicle exhaust, coal combustion, and biomass combustion, all of which accounted for a small proportion of emission factors. The second category includes EC1, and the third category includes OC3, reflecting emissions from human sources, vehicle emissions, and road dust. Emission factors for categories 2 and 3 are more significant. In Figure 11b, the cluster analysis figure of sampling area B does not classify EC1 as a separate category, but it can be seen from Figure 8 that EC1 at sampling area B is not significantly different from other areas, which may be influenced by the very high OC3 content in this area. It is pointed out that OC3 is one of the characteristic carbon components of anthropogenic emission sources such as cooking fumes [56]. Therefore, it is suggested, in this study, that human activities such as smoking and cooking at sampling area B is the reason for the correlation deviation between carbon fractions in its cluster analysis.

3.3.2. Source Analysis of Carbon Fractions Based on Principal Component Analysis (PCA)

In this study, IBM SPSS Statistics 27 was used for principal component analysis of carbon fractions. The results of the model operation showed a KMO value > 0.6 and a significant value < 0.001 in the Bartlett spherical test, indicating that the data were suitable for PCA. The principal fraction orthogonal rotation factor load matrix is shown in Table 3.

Table 3. PCA load results of dust samples.

| Fraction | Factor1 | Factor2 | Factor3 |
|---------------------------------------|--------------|--------------|--------------|
| OC1 | 0.208 | 0.756 | 0.543 |
| OC2 | 0.711 | 0.307 | −0.037 |
| OC3 | 0.822 | −0.159 | −0.456 |
| OC4 | 0.768 | 0.281 | −0.459 |
| EC1 | 0.907 | 0.089 | 0.022 |
| EC2 | 0.731 | −0.212 | 0.583 |
| EC3 | 0.582 | −0.663 | 0.433 |
| Eigenvalue | 3.510 | 1.263 | 1.166 |
| Variance contribution rate | 50.141 | 18.036 | 16.664 |
| Cumulative variance contribution rate | 50.141 | 68.178 | 84.841 |

As shown in Table 3, the PCA load result of carbon fractions in mixed dust samples from Nanchang City revealed that factor 1 was highly loaded with OC2, OC3, OC4, and EC1, which are markers for coal burning, road dust, and cooking fumes. This factor represented a mixed emission source involving coal burning, gasoline motor vehicle exhaust, and human sources [19,56]. Factor 2 was an obvious biomass burning factor because it contained a high loading of the OC1 fraction, which is the hallmark of biomass burning [57]. The high load fractions of factor 3 were EC2 and EC3, which were markers of diesel vehicle emissions [31], so factor 3 represented diesel exhaust. These three factors explained 84.8% of the sources with high reliability.

In summary, the source analysis results based on PCA showed that the main contributing sources of carbon fractions in dust from Nanchang City were combustion sources

(coal burning, biomass burning, etc.), vehicle exhaust sources (gasoline and diesel vehicles exhaust), and human sources (cooking fumes, cigarette smoking, etc.).

4. Strength and Limitations

In this paper, we investigated the distribution of dust particle size and carbon fractions in Nanchang, a typical city in central China, and explored the main emission sources using cluster analysis and principal component analysis to provide a reference for understanding the emission situation in such areas. In addition, we discussed the distribution of dust particle size at different distances from the road and heights from the ground, as well as the distribution of carbon fraction over time in the fall, which can provide some reference value in practical human applications (e.g., location and floor of house selection). However, the limitation of this article is that it does not reveal the impacts of pollution sources on the human body and potential health risks based on differences in particle size distributions and carbon compositions. We may explore this aspect in depth in the future. Moreover, the time-series sampling duration in this paper is only three months in the fall, which is not enough to fully understand the changes in carbon fractions over time under various conditions. We can enrich the experimental conclusions by prolonging the sampling duration or supplementing with related experiments in other seasons in the future.

5. Conclusions

Particle size distribution of dust in four residential areas and three road sampling points in Nanchang City and the effects of distance and height from the source on particle size were studied. The sources of carbon components in dust were identified based on the distribution of carbon components. The distribution of dust particle size in different sampling areas was similar, with particles larger than 10 μm accounting for the majority (over 69.8%). Dust particle size showed a decreasing trend with increasing horizontal distance from the main road and vertical height from the ground. Indoor and outdoor dust had similar particle size distributions, but anthropogenic activities significantly affected the particle size distribution of indoor dust.

The distribution of OC and EC in the dust at different sampling areas varied, and there were certain differences between indoor and outdoor dust in the same area. EC in road dust (22.9–44.8 mg/g) was higher than that in residential dust (18.6–21.4 mg/g), and EC outdoors (7.8–34.5 mg/g) was higher than EC indoors (9.9–24.3 mg/g) in the same area. OC content in indoor dust in residential areas was higher than that in atmospheric dust when there were obvious indoor OC emission sources. Indoor environments and behaviors such as smoking, cooking, and lack of indoor ventilation led to higher OC content in indoor dust. The order of the percentages of carbon fractions in dust was $\text{OC}_3 > \text{EC}_1 > \text{EC}_2 \& \text{OC}_4 > \text{EC}_3 \& \text{OC}_1$ in residential areas and $\text{EC}_2 > \text{OC}_3 > \text{EC}_1 \& \text{OC}_4 > \text{OC}_2 > \text{EC}_3 \& \text{OC}_1$ in road dust mainly originating from vehicle exhaust. There were slight differences in carbon fractions between indoor and outdoor dust in residential areas, showing that OC_3 in indoor dust was significantly affected by indoor human activities (smoking, etc.) and EC_1 in outdoor dust was significantly affected by motor vehicle exhaust. The ratio of OC/EC and SOC in dust decreased from autumn to winter. SOC in dust from Nanchang was at a medium level compared to SOC results reported in other cities/regions around the world.

The combination of cluster analysis and principal component analysis showed that the sources of carbon components in the dust from Nanchang were basically stable, mainly originating from combustion sources, vehicle exhaust sources, and human sources.

Author Contributions: Conceptualization, H.H., Z.H. and C.Z.; software, Z.H. and Y.T.; validation, H.H., Z.H. and C.Z.; data curation, H.H. and Z.H.; writing—original draft preparation, H.H., Z.H. and C.Z.; writing—review and editing, H.H., Z.H., Y.T., C.Y., J.L. and F.Z.; supervision, H.H. and C.Z.; funding acquisition, H.H., J.L. and C.Y. All authors have read and agreed to the published version of the manuscript.

Funding: This work was supported by the National Natural Science Foundation of China (42265011, 52064037), the Cultivating Project for Academic and Technical Leader of Key Discipline of Jiangxi Province (20225BCJ23027, 20212BCJL23054), and Open Fund project for Key Laboratory of Poyang Lake Environment and Resource Q3 Utilization of Ministry of Education (2022Y01).

Institutional Review Board Statement: Not applicable.

Informed Consent Statement: Not applicable.

Data Availability Statement: The data presented in this study are contained within the article.

Conflicts of Interest: The authors declare no conflicts of interest. The funders had no role in the design of the study; in the collection, analyses, or interpretation of data; in the writing of the manuscript, or in the decision to publish the results.

References

1. Li, M.; Yu, S.; Chen, X.; Li, Z.; Zhang, Y.; Song, Z.; Liu, W.; Li, P.; Zhang, X.; Zhang, M.; et al. Impacts of condensable particulate matter on atmospheric organic aerosols and fine particulate matter (PM_{2.5}) in China. *Atmos. Chem. Phys.* **2022**, *22*, 11845–11866. [CrossRef]
2. State Council of the People's Republic of China. Three-Year Action Plan of Win the Blue Sky Defence War 2018. Beijing. 2018. Available online: https://www.gov.cn/zhengce/content/2018-07/03/content_5303158.htm (accessed on 27 June 2018).
3. State Council of the People's Republic of China. Air Pollution Prevention and Control Action Plan 2013. Beijing. 2013. Available online: https://www.gov.cn/zwggk/2013-09/12/content_2486773.htm (accessed on 10 September 2013).
4. Yin, Z.; Duan, M.; Li, Y.; Xu, T.; Wang, H. Predicting gridded winter PM_{2.5} concentration in the east of China. *Atmos. Chem. Phys.* **2022**, *22*, 11173–11185. [CrossRef]
5. Song, T.; Feng, M.; Song, D.; Liu, S.; Tan, Q.; Wang, Y.; Luo, Y.; Chen, X.; Yang, F. Comparative Analysis of Secondary Organic Aerosol Formation during PM_{2.5} Pollution and Complex Pollution of PM_{2.5} and O₃ in Chengdu, China. *Atmosphere* **2022**, *13*, 1834.
6. Soheili, F.; Woodward, S.; Abdul-Hamid, H.; Naji, H.R. The Effect of Dust Deposition on the Morphology and Physiology of Tree Foliage. *Water Air Soil Pollut.* **2023**, *234*, 339. [CrossRef]
7. Lanzerstorfer, C. Variations in the composition of house dust by particle size. *J. Environ. Sci. Health Part A* **2017**, *52*, 770–777. [CrossRef] [PubMed]
8. Lee, K.Y.; Batmunkh, T.; Joo, H.S.; Park, K. Comparison of the physical and chemical characteristics of fine road dust at different urban sites. *J. Air Waste Manag. Assoc.* **2018**, *68*, 812–823. [CrossRef]
9. Dai, Q.; Bi, X.; Huangfu, Y.; Yang, J.; Li, T.; Khan, J.Z.; Song, C.; Xu, J.; Wu, J.; Zhang, Y.; et al. A size-resolved chemical mass balance (SR-CMB) approach for source apportionment of ambient particulate matter by single element analysis. *Atmos. Environ.* **2019**, *197*, 45–52. [CrossRef]
10. Lin, Y.; Mu, G.; Zhao, X.; Xu, L.; Zhang, J. Atmospheric dustfall exhibits consistent sedimentary sorting with height evidenced by grain size characteristics. *Sci. Total Environ.* **2023**, *864*, 161143. [CrossRef]
11. Gupta, G.P.; Kumar, B.; Singh, S.; Kulshrestha, U.C. Urban climate and its effect on biochemical and morphological characteristics of Arjun (*Terminalia arjuna*) plant in National Capital Region Delhi. *Chem. Ecol.* **2015**, *31*, 524–538. [CrossRef]
12. Bibi, M.; Saad, M.; Masmoudi, M.; Laurent, B.; Alfaro, S.C. Long-term (1980–2018) spatial and temporal variability of the atmospheric dust load and deposition fluxes along the North-African coast of the Mediterranean Sea. *Atmos. Res.* **2020**, *234*, 104689. [CrossRef]
13. Elperin, T.; Fominykh, A.; Katra, I.; Krasovtsov, B. Modelling of nitric acid gas adsorption by atmospheric dust particles. *Aerosol Sci. Technol.* **2019**, *53*, 381–393. [CrossRef]
14. Han, Y.; Zhu, T.; Guan, T.; Zhu, Y.; Liu, J.; Ji, Y.; Gao, S.; Wang, F.; Lu, H.; Huang, W. Association between size-segregated particles in ambient air and acute respiratory inflammation. *Sci. Total Environ.* **2016**, *565*, 412–419. [CrossRef] [PubMed]
15. Tétreault, L.-F.; Doucet, M.; Gamache, P.; Fournier, M.; Brand, A.; Kosatsky, T.; Smargiassi, A. Childhood Exposure to Ambient Air Pollutants and the Onset of Asthma: An Administrative Cohort Study in Québec. *Environ. Health Perspect.* **2016**, *124*, 1276–1282. [CrossRef] [PubMed]
16. Luo, P.; Bao, L.-J.; Guo, Y.; Li, S.-M.; Zeng, E.Y. Size-dependent atmospheric deposition and inhalation exposure of particle-bound organophosphate flame retardants. *J. Hazard. Mater.* **2016**, *301*, 504–511. [CrossRef] [PubMed]
17. Downward, G.S.; van Nunen, E.J.; Kerckhoffs, J.; Vineis, P.; Brunekreef, B.; Boer, J.M.; Messier, K.P.; Roy, A.; Verschuren, W.M.M.; van der Schouw, Y.T.; et al. Long-Term Exposure to Ultrafine Particles and Incidence of Cardiovascular and Cerebrovascular Disease in a Prospective Study of a Dutch Cohort. *Environ. Health Perspect.* **2018**, *126*, 127007. [CrossRef] [PubMed]
18. Zhang, R.; Zhang, X.; Gao, S.; Liu, R. Assessing the in vitro and in vivo toxicity of ultrafine carbon black to mouse liver. *Sci. Total Environ.* **2019**, *655*, 1334–1341. [CrossRef]
19. Liu, X.; Kong, S.; Yan, Q.; Liu, H.; Wang, W.; Chen, K.; Yin, Y.; Zheng, H.; Wu, J.; Qin, S.; et al. Size-segregated carbonaceous aerosols emission from typical vehicles and potential depositions in the human respiratory system. *Environ. Pollut.* **2020**, *264*, 114705. [CrossRef]

20. Li, Z.; Ju, S.; Duan, M.; Cai, S. Quantitative Selection of Leading Industries of Green Economy in Coastal Cities Based on Industrial Relevance. *J. Coast. Res.* **2020**, *103* (Suppl. S1), 566. [CrossRef]
21. Li, Y.; Zhao, B.; Duan, K.; Cai, J.; Niu, W.; Dong, X. Assessments of Water-Soluble Inorganic Ions and Heavy Metals in Atmospheric Dustfall and Topsoil in Lanzhou, China. *Int. J. Environ. Res. Public Health* **2020**, *17*, 2970. [CrossRef]
22. Meng, L.; Zhao, T.; He, Q.; Yang, X.; Mantimin, A.; Wang, M.; Pan, H.; Huo, W.; Yang, F.; Zhou, C. Dust Radiative Effect Characteristics during a Typical Springtime Dust Storm with Persistent Floating Dust in the Tarim Basin, Northwest China. *Remote Sens.* **2022**, *14*, 1167. [CrossRef]
23. Tan, Z.; Ma, M.; Huang, W.; Tan, C.; Zhao, Z.; Ding, F. Study on dust occurrence and transportation related to boundary layer height in Northwest China. *Atmos. Sci. Lett.* **2022**, *23*, e1083. [CrossRef]
24. Zhang, F.; Zhang, L.; Pan, M.; Zhong, X.; Zhao, E.; Wang, Y.; Du, C. Black carbon and mineral dust in snow cover across a typical city of Northeast China. *Sci. Total Environ.* **2022**, *807*, 150397. [CrossRef] [PubMed]
25. Zhang, Z.; Wang, Y.; Tan, F.; Bao, M.; Zhang, L.; Rodgers, T.F.; Chen, J. Characteristics and risk assessment of organophosphorus flame retardants in urban road dust of Dalian, Northeast China. *Sci. Total Environ.* **2020**, *705*, 135995. [CrossRef] [PubMed]
26. Chen, Y.; Du, W.; Chen, J.; Hong, Y.; Zhao, J.; Xu, L.; Xiao, H. Chemical composition, structural properties, and source apportionment of organic macromolecules in atmospheric PM10 in a coastal city of Southeast China. *Environ. Sci. Pollut. Res.* **2017**, *24*, 5877–5887. [CrossRef] [PubMed]
27. Wang, Q.; Feng, W.; Liu, M.; Xu, H. Atmospheric elemental carbon deposition from urban and suburban sites of Shanghai: Characteristics, sources and comparison with aerosols and soils. *Atmos. Pollut. Res.* **2021**, *12*, 193–199. [CrossRef]
28. Zhao, L.; Yu, R.; Yan, Y.; Cheng, Y.; Hu, G.; Huang, H. Bioaccessibility and provenance of heavy metals in the park dust in a coastal city of southeast China. *Appl. Geochem.* **2020**, *123*, 104798. [CrossRef]
29. Zou, C.; Wang, J.; Gao, Y.; Huang, H. Distribution characteristics and optical properties of carbonaceous aerosol: Brown carbon and black carbon in Nanchang, inland China. *Atmos. Pollut. Res.* **2023**, *14*, 101700. [CrossRef]
30. Nanchang Municipal Bureau of Ecology and Environment. Data Table of Traffic Flow and Noise Monitoring of Various Roads in Nanchang. Nanchang. 2021. Available online: <https://sthjj.nc.gov.cn/ncgjbj/zsjcbg/202112/6908b76094184f569c2f91d11929c640.shtml> (accessed on 6 December 2021).
31. Demir, T.; Yenisoy-Karakaş, S.; Karakaş, D. PAHs, elemental and organic carbons in a highway tunnel atmosphere and road dust: Discrimination of diesel and gasoline emissions. *Build. Environ.* **2019**, *160*, 106166. [CrossRef]
32. Chu, G.; Sun, Q.; Zhaoyan, G.; Rioual, P.; Qiang, L.; Kaijun, W.; Han, J.; Liu, J. Dust records from varved lacustrine sediments of two neighboring lakes in northeastern China over the last 1400 years. *Quat. Int.* **2009**, *194*, 108–118. [CrossRef]
33. Han, Y.; Cao, J.; Chow, J.C.; Watson, J.G.; An, Z.; Jin, Z.; Fung, K.; Liu, S. Evaluation of the thermal/optical reflectance method for quantification of elemental carbon in sediments. *Chemosphere* **2007**, *69*, 526–533. [CrossRef]
34. Chow, J.C.; Watson, J.G.; Green, M.C.; Wang, X.; Chen, L.-W.A.; Trimble, D.L.; Cropper, P.M.; Kohl, S.D. Separation of brown carbon from black carbon for IMPROVE and Chemical Speciation Network PM_{2.5} samples. *J. Air Waste Manag. Assoc.* **2018**, *68*, 494–510. [CrossRef] [PubMed]
35. Papaefstathiou, E.; Bezantakos, S.; Stylianou, M.; Biskos, G.; Agapiou, A. Comparison of particle size distributions and volatile organic compounds exhaled by e-cigarette and cigarette users. *J. Aerosol Sci.* **2020**, *141*, 105487. [CrossRef]
36. Gondwal, T.K.; Mandal, P. Review on Classification, Sources and Management of Road Dust and Determination of Uncertainty Associated with Measurement of Particle Size of Road Dust. *MAPAN* **2021**, *36*, 909–924. [CrossRef]
37. Li, N.; Wei, X.; Han, W.; Sun, S.; Wu, J. Characteristics and temporal variations of organic and elemental carbon aerosols in PM1 in Changchun, Northeast China. *Environ. Sci. Pollut. Res.* **2020**, *27*, 8653–8661. [CrossRef]
38. Ruprecht, A.A.; De Marco, C.; Saffari, A.; Pozzi, P.; Mazza, R.; Veronese, C.; Angellotti, G.; Munarini, E.; Ogliari, A.C.; Westerdahl, D.; et al. Environmental pollution and emission factors of electronic cigarettes, heat-not-burn tobacco products, and conventional cigarettes. *Aerosol Sci. Technol.* **2017**, *51*, 674–684. [CrossRef]
39. Chen, P.; Kang, S.; Li, C.; Hu, Z.; Tripathee, L.; Rai, M.; Pu, T.; Yin, X.; Gustafsson, O. Carbonaceous aerosol transport from the Indo-Gangetic Plain to the Himalayas: Carbon isotope evidence and light absorption characteristics. *Geosci. Front.* **2023**, *14*, 101516. [CrossRef]
40. Zhang, Q.; Sarkar, S.; Wang, X.; Zhang, J.; Mao, J.; Yang, L.; Shi, Y.; Jia, S. Evaluation of factors influencing secondary organic carbon (SOC) estimation by CO and EC tracer methods. *Sci. Total Environ.* **2019**, *686*, 915–930. [CrossRef]
41. Mbengue, S.; Fusek, M.; Schwarz, J.; Vodička, P.; Šmejkalová, A.H.; Holoubek, I. Four years of highly time resolved measurements of elemental and organic carbon at a rural background site in Central Europe. *Atmos. Environ.* **2018**, *182*, 335–346. [CrossRef]
42. Sun, J.; Liang, M.; Shi, Z.; Shen, F.; Li, J.; Huang, L.; Ge, X.; Chen, Q.; Sun, Y.; Zhang, Y.; et al. Investigating the PM_{2.5} mass concentration growth processes during 2013–2016 in Beijing and Shanghai. *Chemosphere* **2019**, *221*, 452–463. [CrossRef]
43. Wu, C.; Wu, D.; Yu, J.Z. Quantifying black carbon light absorption enhancement with a novel statistical approach. *Atmos. Chem. Phys.* **2018**, *18*, 289–309. [CrossRef]
44. Wu, C.; Yu, J.Z. Determination of primary combustion source organic carbon-to-elemental carbon (OC/EC) ratio using ambient OC and EC measurements: Secondary OC-EC correlation minimization method. *Atmos. Chem. Phys.* **2016**, *16*, 5453–5465. [CrossRef]
45. Porter, W.C.; Jimenez, J.L.; Barsanti, K.C. Quantifying Atmospheric Parameter Ranges for Ambient Secondary Organic Aerosol Formation. *ACS Earth Space Chem.* **2021**, *5*, 2380–2397. [CrossRef]

46. Wu, C.; Wu, D.; Yu, J.Z. Estimation and Uncertainty Analysis of Secondary Organic Carbon Using 1 Year of Hourly Organic and Elemental Carbon Data. *J. Geophys. Res. Atmos.* **2019**, *124*, 2774–2795. [[CrossRef](#)]
47. Moretti, S.; Tassone, A.; Andreoli, V.; Carbone, F.; Pirrone, N.; Sprovieri, F.; Naccarato, A. Analytical study on the primary and secondary organic carbon and elemental carbon in the particulate matter at the high-altitude Monte Curcio GAW station, Italy. *Environ. Sci. Pollut. Res.* **2021**, *28*, 60221–60234. [[CrossRef](#)] [[PubMed](#)]
48. Qi, M.; Jiang, L.; Liu, Y.; Xiong, Q.; Sun, C.; Li, X.; Zhao, W.; Yang, X. Analysis of the Characteristics and Sources of Carbonaceous Aerosols in PM_{2.5} in the Beijing, Tianjin, and Langfang Region, China. *Int. J. Environ. Res. Public Health* **2018**, *15*, 1483. [[CrossRef](#)] [[PubMed](#)]
49. Huang, Y.; Zhang, L.; Li, T.; Chen, Y.; Yang, F. Seasonal Variation of Carbonaceous Species of PM_{2.5} in a Small City in Sichuan Basin, China. *Atmosphere* **2020**, *11*, 1286. [[CrossRef](#)]
50. Ram, K.; Sarin, M.; Hegde, P. Atmospheric abundances of primary and secondary carbonaceous species at two high-altitude sites in India: Sources and temporal variability. *Atmos. Environ.* **2008**, *42*, 6785–6796. [[CrossRef](#)]
51. Yu, X.-Y.; Cary, R.A.; Laulainen, N.S. Primary and secondary organic carbon downwind of Mexico City. *Atmos. Chem. Phys.* **2009**, *9*, 6793–6814. [[CrossRef](#)]
52. Wang, C.; Hui, F.; Wang, Z.; Zhu, X.; Zhang, X. Chemical characteristics of size-fractionated particles at a suburban site in Shijiazhuang, North China: Implication of secondary particle formation. *Atmos. Res.* **2021**, *259*, 105680. [[CrossRef](#)]
53. Ji, X.; Ji, W. Determination of the Volatile Organic Compounds (VOCs) in Mature and Immature Foliage of Five Species of Pinaceae by Gas Chromatography–Mass Spectrometry (GC-MS) with Principal Component Analysis (PCA) and Cluster Analysis (CA). *Anal. Lett.* **2022**, *55*, 1412–1424. [[CrossRef](#)]
54. Li, H.Z.; Dallmann, T.R.; Li, X.; Gu, P.; Presto, A.A. Urban Organic Aerosol Exposure: Spatial Variations in Composition and Source Impacts. *Environ. Sci. Technol.* **2018**, *52*, 415–426. [[CrossRef](#)] [[PubMed](#)]
55. Wang, P.; Hu, J.; Han, G.; Liu, T.; Ma, W.-M.; Li, J. Preliminary investigation of soil organic carbon distribution and turnover patterns, and potential pollution sources in and around a typical coking plant in North China. *Environ. Res.* **2023**, *228*, 115845. [[CrossRef](#)]
56. Chen, Q.; Sun, H.; Mu, Z.; Wang, Y.; Li, Y.; Zhang, L.; Wang, M.; Zhang, Z. Characteristics of environmentally persistent free radicals in PM_{2.5}: Concentrations, species and sources in Xi'an, Northwestern China. *Environ. Pollut.* **2019**, *247*, 18–26. [[CrossRef](#)] [[PubMed](#)]
57. Koçak, E.; Kılavuz, S.A.; Öztürk, F.; İmamoğlu, İ.; Tuncel, G. Characterization and source apportionment of carbonaceous aerosols in fine particles at urban and suburban atmospheres of Ankara, Turkey. *Environ. Sci. Pollut. Res.* **2021**, *28*, 25701–25715. [[CrossRef](#)] [[PubMed](#)]

Disclaimer/Publisher's Note: The statements, opinions and data contained in all publications are solely those of the individual author(s) and contributor(s) and not of MDPI and/or the editor(s). MDPI and/or the editor(s) disclaim responsibility for any injury to people or property resulting from any ideas, methods, instructions or products referred to in the content.